



HAL
open science

A New Pharmacokinetic-Pharmacodynamic Model To Characterize the Inoculum Effect of *Acinetobacter baumannii* on Polymyxin B In Vitro

Grace Akrong, Alexia Chauzy, Vincent Aranzana-Climent, Mathilde Lacroix, Luc Deroche, Laure Prouvensier, Julien Buyck, William Couet, Sandrine Marchand

► **To cite this version:**

Grace Akrong, Alexia Chauzy, Vincent Aranzana-Climent, Mathilde Lacroix, Luc Deroche, et al.. A New Pharmacokinetic-Pharmacodynamic Model To Characterize the Inoculum Effect of *Acinetobacter baumannii* on Polymyxin B In Vitro. *Antimicrobial Agents and Chemotherapy*, 2022, 66 (1), 10.1128/AAC.01789-21 . hal-03615758

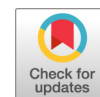
HAL Id: hal-03615758

<https://hal.science/hal-03615758>




Submitted on 10 Jul 2024

HAL is a multi-disciplinary open access archive for the deposit and dissemination of scientific research documents, whether they are published or not. The documents may come from teaching and research institutions in France or abroad, or from public or private research centers.

L'archive ouverte pluridisciplinaire **HAL**, est destinée au dépôt et à la diffusion de documents scientifiques de niveau recherche, publiés ou non, émanant des établissements d'enseignement et de recherche français ou étrangers, des laboratoires publics ou privés.



A New Pharmacokinetic-Pharmacodynamic Model To Characterize the Inoculum Effect of *Acinetobacter baumannii* on Polymyxin B *In Vitro*

Grace Akrong,^{a,b} Alexia Chauzy,^{a,b} Vincent Aranzana-Climent,^{a,b,c} Mathilde Lacroix,^{a,b,d} Luc Deroche,^{a,b} Laure Prouvensier,^{a,e}
 Julien M. Buyck,^{a,b}  William Couet,^{a,b,e}  Sandrine Marchand^{a,b,e}

^aINSERM U1070, Poitiers, France

^bUniversité de Poitiers, Poitiers, France

^cPharmacometrics, Department of Pharmacy, Uppsala University, Uppsala, Sweden

^dInstitut ROCHE, Boulogne-Billancourt, France

^eDépartement de Toxicologie et de Pharmacocinétique, CHU de Poitiers, Poitiers, France

ABSTRACT The inoculum effect (i.e., reduction in antimicrobial activity at large starting inoculum) is a phenomenon described for various pathogens. Given that limited data exist regarding inoculum effect of *Acinetobacter baumannii*, we evaluated killing of *A. baumannii* by polymyxin B, a last-resort antibiotic, at several starting inocula and developed a pharmacokinetic-pharmacodynamic (PKPD) model to capture this phenomenon. *In vitro* static time-kill experiments were performed using polymyxin B at concentrations ranging from 0.125 to 128 mg/L against a clinical *A. baumannii* isolate at four starting inocula from 10⁵ to 10⁸ CFU/mL. Samples were collected up to 30 h to quantify the viable bacterial burden and were simultaneously modeled in the NONMEM software program. The expression of polymyxin B resistance genes (*lpxACD*, *pmrCAB*, and *wzc*), and genetic modifications were studied by RT-qPCR and DNA sequencing experiments, respectively. The PKPD model included a single homogeneous bacterial population with adaptive resistance. Polymyxin B effect was modeled as a sigmoidal E_{max} model and the inoculum effect as an increase of polymyxin B EC₅₀ with increasing starting inoculum using a power function. Polymyxin B displayed a reduced activity as the starting inoculum increased: a 20-fold increase of polymyxin B EC₅₀ was observed between the lowest and the highest inoculum. No effects of polymyxin B and inoculum size were observed on the studied genes. The proposed PKPD model successfully described and predicted the pronounced *in vitro* inoculum effect of *A. baumannii* on polymyxin B activity. These results should be further validated using other bacteria/antibiotic combinations and *in vivo* models.

KEYWORDS *A. baumannii*, PKPD model, inoculum effect, polymyxin B

It is admitted that dense bacterial population may reduce antibiotics efficacy (1, 2). This phenomenon referred as inoculum effect (IE) may have several origins such as greater production of β-lactamases observed with *Escherichia coli* and leading to reduction of effective concentrations of β-lactam antibiotics available for bacterial killing (3), greater biofilm barrier formation in the presence of higher *E. coli* bacterial density (4), or larger release of lipopolysaccharides (LPS) reducing *Pseudomonas aeruginosa* susceptibility to colistin (5). IE has been described for various pathogens such as *Staphylococcus aureus*, *P. aeruginosa* and *Enterobacter* species (*E. coli*, *Klebsiella pneumoniae*) (3, 6, 7). IE may obviously have an effect on treatment efficacy and antibiotic dosing regimen selection, especially in the case of difficult-to-treat infections with high burden load including endocarditis, meningitis, abscesses, and other deep-seated

Copyright © 2022 American Society for Microbiology. All Rights Reserved.

Address correspondence to Sandrine Marchand, sandrine.marchand@univ-poitiers.fr.

The authors declare no conflict of interest.

Received 9 September 2021

Returned for modification 6 October 2021

Accepted 6 November 2021

Accepted manuscript posted online

15 November 2021

Published 18 January 2022

infections (8). Although, an increase of MIC with inoculum has been observed on several occasions (3, 9), IE is not taken into consideration by regulators because EUCAST and CLSI guidelines rely on MIC determinations at a unique starting inoculum of 5×10^5 CFU/ml for PK/PD breakpoints determination (10, 11).

IE has often been attested by an 8-fold or more increase of MIC when the starting inoculum increases from 5×10^5 to 5×10^7 CFU/mL (8, 12–14), whereas more informative pharmacokinetic-pharmacodynamic (PKPD) modeling approaches have only been used on few occasions (4, 15–18). Mechanism-based PKPD models were initially developed and validated by J. Bulitta and colleagues. to capture the IE of *P. aeruginosa* on ceftazidime (17) and then colistin (18) effects. Concomitantly, a semi-mechanistic model was published by Bhagunde et al. describing the IE of *E. coli* on piperacillin activity (4). Although very elegant, these PKPD models relying on mechanistic assumptions are species dependent and may not apply to all sorts of antibiotics/bacteria combinations. Therefore, our objective was to develop a mechanism independent PKPD model with potential large application. *Acinetobacter baumannii* was selected for this study as a strain responsible for difficult-to-treat pulmonary infections with potentially high burden load (19), but also because, to our knowledge, *A. baumannii* is a pathogen for which the IE has never been characterized. And polymyxin B (PMB) was chosen as a last resort antibiotic potentially active against *A. baumannii* (20).

RESULTS

MIC determinations. MIC values were <0.125, 0.125, 0.25, and 1 mg/L for the 10^5 , 10^6 , 10^7 , and 10^8 inoculum, respectively.

Time-kill curves experiments. The results of the time-kill experiments are represented as circles in Fig. 1. No PMB effect was observed for concentrations below or equal to 1 mg/L with the inocula of 10^5 , 10^7 , and 10^8 CFU/mL. For a starting inoculum of 10^5 CFU/mL, a PMB concentration of 4 mg/L resulted in a rapid bacterial decay to undetectable CFU within few hours (<3 h) whereas bacterial killing was less pronounced, and regrowth occurred for the other three starting inocula (Fig. 1, circles). Up to 32-fold-higher concentrations were required at a starting inoculum of 10^8 CFU/mL to achieve a similar bactericidal effect. No pre-existing resistant subpopulations growing on PMB-containing agar plates were observed for all four starting inocula tested.

Pharmacodynamic model and simulations. Time-kill curves (TKC) data were well described by the model depicted in Fig. 2. Parameter estimates with their corresponding uncertainties are summarized in Table 1. VPCs of the final model are shown in Fig. 1 and GOF plots in Fig. S1.

Bactericidal effect of PMB (K_{PMB}) was best described by a sigmoidal Emax model (equation 1).

$$K_{PMB} = \frac{E_{max} \times C_{PMB}^{\gamma}}{EC_{50}^{\gamma} + C_{PMB}^{\gamma}} \quad (1)$$

where E_{max} (h^{-1}) is the maximum kill constant; EC_{50} (mg/L) is the PMB concentration that results in 50% of E_{max} ; C_{PMB} is the PMB concentration, and γ is the Hill coefficient that characterizes the steepness of the drug effect relationship. The emergence of adaptive resistance during the experiment was characterized by a transfer rate constant (K_{on}) of nonadapted to adapted bacteria which was not dependent on PMB concentration. Random variability between experiments was included on K_{on} to catch the variability in the bacterial response to PMB from one replicate to another (Table 1). The introduction of interexperiment variability on K_{on} was associated with a decrease in the objective function value (529 versus 341) and the residual error (1.64 vs 0.61 \log_{10} CFU/mL). The impact of adaptive resistance on PMB antibacterial effect was best described as a reduction of PMB $E_{max(0)}$ (initial E_{max} value before adaptive resistance has developed) with time following a linear function (K_{adapt}) (equation 2).

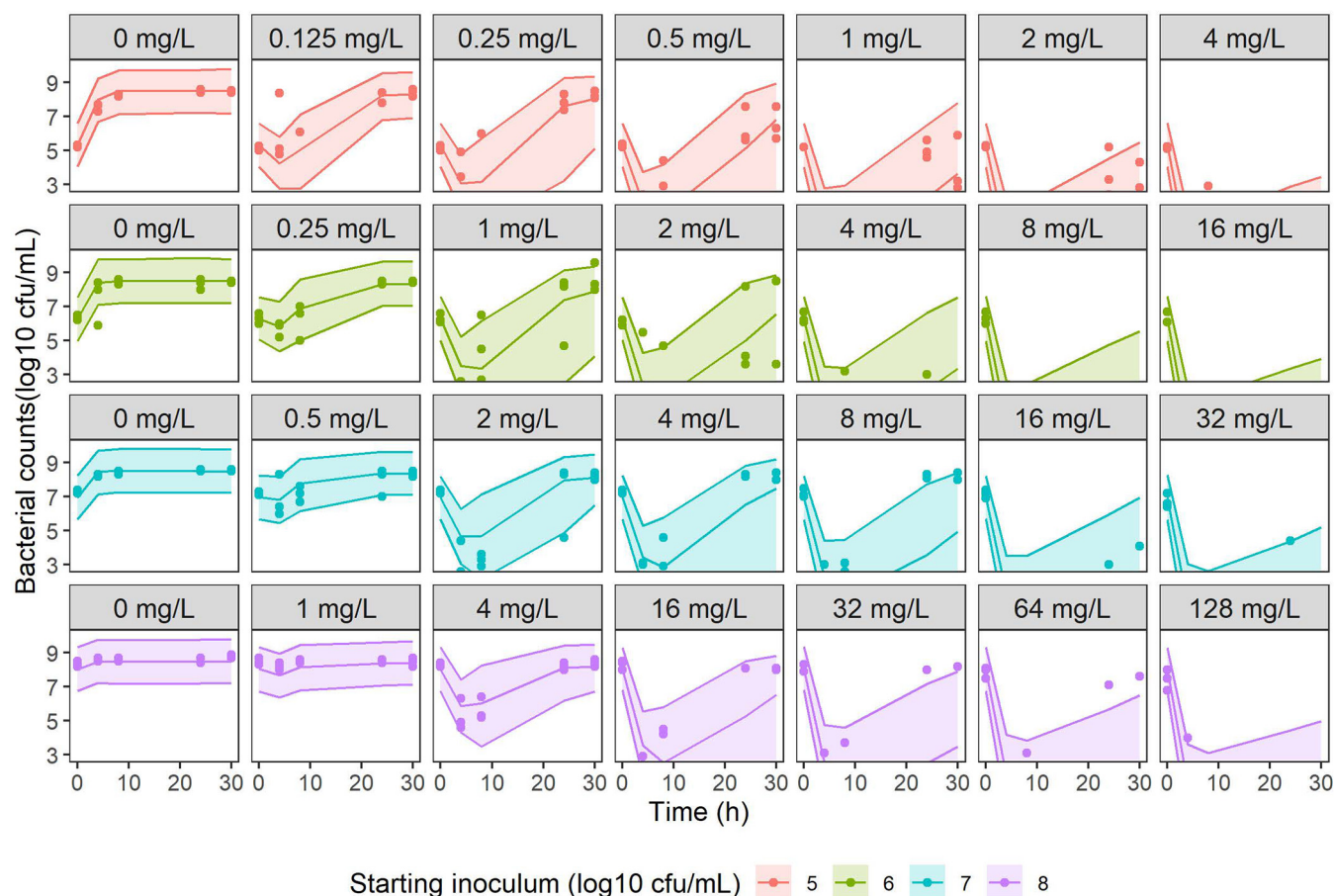


FIG 1 Visual predictive checks (VPC) for the final model. Circles represent experimental data, solid lines depict the median of simulated data and, colored areas depict the 90% prediction interval for 1,000 simulated profiles.

$$E_{max} = E_{max(0)} \times (1 - K_{adapt} \times AR_{on}) \tag{2}$$

The PD model predicted that the percentage of AR_{on} would increase with time from 0% at time 0 to 64%, 87%, and 100% at 4 h, 8 h, and 24 h of the experiment, respectively. Consequently, E_{max} would decrease from its initial value (8.96 h^{-1}) to 4.23 h^{-1} , 2.54 h^{-1} , and 1.58 h^{-1} after 4 h, 8 h, and 24 h of the experiment, respectively, explaining regrowth observed during TKC experiments.

IE was integrated in the model as an increase of PMB EC_{50} with increasing theoretical starting inoculum using a power function (equation 3).

$$EC_{50} = EC_{50,med} \times \left(\frac{\text{Starting inoculum}}{6.5} \right)^\beta \tag{3}$$

where $EC_{50,med}$ is the EC_{50} for a TKC with a theoretical starting inoculum of $10^{6.5}$ CFU/mL and β the coefficient describing the IE on EC_{50} .

PMB bactericidal effect, adaptive resistance effect, and IE were incorporated in the logistic growth model to describe the time course of bacterial counts, such as:

$$\frac{dB}{dt} = Kg \times \left(1 - \frac{B}{Bmax} \right) \times B - \frac{(E_{max(0)} \times (1 - K_{adapt} \times AR_{on})) \times C_{PMB}^y}{EC_{50,med} \times \left(\frac{\text{Starting inoculum}}{6.5} \right)^\beta + C_{PMB}^y} \times B \tag{4}$$

where B (CFU/mL) is the susceptible bacterial population, $Kg \text{ (h}^{-1}\text{)}$ is the apparent growth rate constant, and Bmax (CFU/mL) is the maximum bacterial count reached in the system.

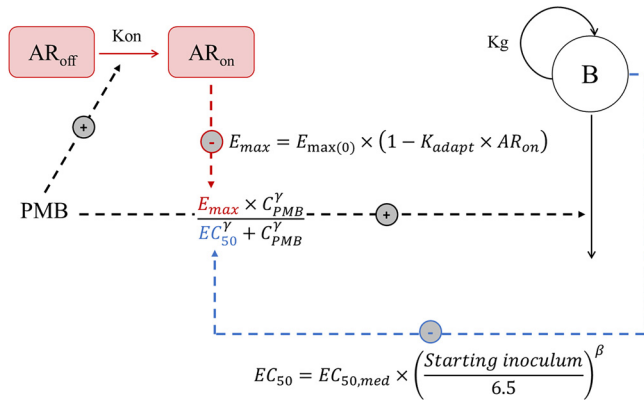


FIG 2 Schematic diagram of the PD final model. Bacteria multiplied with a first-order rate constant (K_g) in the bacterial compartment (B). Polymyxin B (PMB) effect K_{PMB} was modeled according to an E_{max} model. Adaptive resistance (AR) to PMB occurred when bacteria were exposed to PMB according to a first order rate constant K_{on} .

An increase of PMB EC_{50} by a factor of 20 was predicted between the lowest and the highest inocula ($EC_{50} = 0.3, 0.9, 2.28,$ and 5.12 mg/L for inoculum of $10^5, 10^6, 10^7$ and 10^8 CFU/mL, respectively). Much higher PMB concentrations would be necessary to observe PMB bactericidal effect against dense bacterial populations as illustrated in simulations of expected bacterial counts versus time for different inocula (Fig. 3). At a concentration corresponding to the MIC of PMB with the study strain (0.25 mg/L), it is observed that the model predicts a decrease followed by a regrowth with the lowest inoculum (10^5 CFU/mL), while at the highest inoculum (10^8 CFU/mL), no effect is predicted. Similarly, at the highest simulated concentration (8 mg/L), a total bactericidal effect is predicted at the lowest inoculum (10^5 CFU/mL), whereas with the highest inoculum (10^8 CFU/mL) a decay followed by a regrowth was predicted by our model. To better illustrate the IE, initial killing half-lives (IK-HL) of various concentrations of PMB (0.25, 0.5, 1, 2, 4, and 8 mg/L) with the four inocula were calculated from equation 1 and are presented in Table 2.

Expression of PMB resistance genes and genetic modifications in PMB resistance genes. Expression of LPS-modifying (*pmrCAB, lpxACD*) and capsule genes (*wzc*) did not differ significantly in *A. baumannii* over time (4 h, 8 h, and 24 h), with or without treatment and between the two inocula tested (10^6 and 10^8 CFU/mL) (Fig. S2). No genetic modification was observed in *pmrCAB, lpxACD, wzc,* and *eptA* genes, with or without treatment and between the two inocula tested (10^6 and 10^8 CFU/mL) (data not shown).

DISCUSSION

This study has demonstrated a strong *in vitro* IE of *A. baumannii* on PMB antimicrobial activity, consistent with those of *P. aeruginosa* on PMB (21) and also colistin (18), previously described. Yet the most innovative aspect of this new study was the development of an original PKPD model. On many occasions, TKC exhibit an initial rapid decay of CFU with time followed by regrowth after few hours (Fig. 1) (16–18). This type of behavior can be described by two types of PKPD models, with either two heterogeneous subpopulations, S for sensitive and R for resistant (S/R model), or a single population with adaptive resistance (AR model). Because of its relative simplicity, formal statistical comparisons frequently favor the S/R model, due to the parsimony principle (22), although this model may not be consistent with the mechanism responsible for regrowth and may be misleading. However, in this study, the tested AR model (Fig. 2) was statistically superior to the S/R model to describe the experimental TKC data. In agreement with that, bacterial susceptibility testing at time 0 failed to demonstrate the presence of a small fraction of R bacteria to support the S/R model. The simultaneous occurrence of IE and adaptive resistance (AR) makes MIC modifications with bacterial density difficult to interpret, whereas PKPD modeling can discriminate between these separate phenomena to describe the CFU versus time curves (Fig. 2). Accordingly, an

TABLE 1 Parameter estimates and relative standard error (RSE) for the final model

Parameter	Unit	Description	Estimate (RSE%)	% CV for IIV (RSE %)
INOC ₈	log ₁₀ CFU/mL	Initial bacterial density for 10 ⁸ CFU/mL inoculum	8.06 (1.1)	-
INOC ₇	log ₁₀ CFU/mL	Initial bacterial density for 10 ⁷ CFU/mL inoculum	6.96 (1.6)	-
INOC ₆	log ₁₀ CFU/mL	Initial bacterial density for 10 ⁶ CFU/mL inoculum	6.29 (1.7)	-
INOC ₅	log ₁₀ CFU/mL	Initial bacterial density for 10 ⁵ CFU/mL inoculum	5.33 (2.2)	-
K _g	h ⁻¹	Apparent growth rate constant	1.62 (8)	-
B _{max}	log ₁₀ CFU/mL	Maximum bacterial count reached in the system	8.5 (0.7)	-
E _{max(0)}	h ⁻¹	Maximum kill rate constant due to PMB when no adaptive resistance has developed	8.96 (9)	-
EC ₅₀	mg/L	PMB concentration that results in 50% of E _{max(0)}	1.46 (9.1)	-
γ		Hill coefficient that characterizes the steepness of the drug effect relationship	0.656 (5.6)	-
K _{on}	h ⁻¹	Rate constant for development of adaptive resistance	0.253 (19.8)	40.8 (17.4)
K _{adapt}		Linear function for impact of adaptive resistance on PMB antibacterial effect	0.824 (2.8)	
β		Inoculum effect	6.04 (11.5)	-
σ	log ₁₀ CFU/mL	Additive residual error on log ₁₀ scale for total bacteria count	0.608 (22)	-

CV, coefficient of variation.

IIV, interindividual variability.

increase of PMB EC₅₀ modeled by a power function was added to the initial AR model to take into account the IE (equation 3). This model presents similarities with that previously proposed by Bhagunde et al., to capture the IE of *E. coli* on piperacillin killing effect, and relying on a reduction of the effective drug concentration available for bacterial killing as the result of a greater biofilm barrier in the presence of higher bacterial density (4). However, biofilm formation is unlikely to occur during *in vitro* time-kill experiments under constant shaking, and for that reason our objective was to develop a non-mechanistic model. However, the model developed by Bhagunde et al. and ours both relate the decrease in killing effect with time to the baseline inoculum, and therefore do not capture the changing antibiotic activity together with changing bacterial density with time during TKC experiments, as previously mentioned by Nielsen and Friberg (23). However, substitution of the starting inoculum term in equation 3, by the changing value of log CFU with time, leads to model unidentifiability, probably due to the appearance log CFU on both sides of the equal sign in equation 4 and interaction thus introduced between the IE, PMB effect, and adaptive resistance parameters.

Noticeably, Nielsen and colleagues have proposed to extend the application of their PD model in which growing bacteria are eventually converted into resting state, initially proposed to describe the biphasic killing behavior sometimes observed during TKC experiments or/and the decrease of growth rate before reaching plateau (24, 25), to investigate IE. This alternative was then successfully tested using *E. coli* and ciprofloxacin and considering two subpopulations of bacteria (S and R), each present in a growing phase possibly converted more or less rapidly into resting state, as a function of the inoculum size (16). However, this model was tested, but without success, to describe our data.

Altogether, our model provided a reasonably good description of the experimental data and offers the advantage of relative simplicity with no mechanistic assumptions. It would now be interesting to assess this model's capability to describe the IE of bacteria producing β-lactamases in the presence of β-lactam antibiotics.

The EC₅₀ values estimated during the present study increased from 0.30 to 5.12 mg/L when the starting inoculum increased from 10⁵ to 10⁸ CFU/mL (Fig. 3). This 17-fold variation suggests a major IE but remains difficult to interpret. Simulations were conducted to better illustrate the consequences of the IE on CFU versus time curves during TKC experiments with PMB concentrations varying between 0.25 and 8 mg/L (Fig. 3), using a range of total concentrations consistent with those encountered in patients (26). The model developed in this study predicted an important reduction of the PMB PD effect in the presence of a dense bacterial population; however, adaptive resistance is a

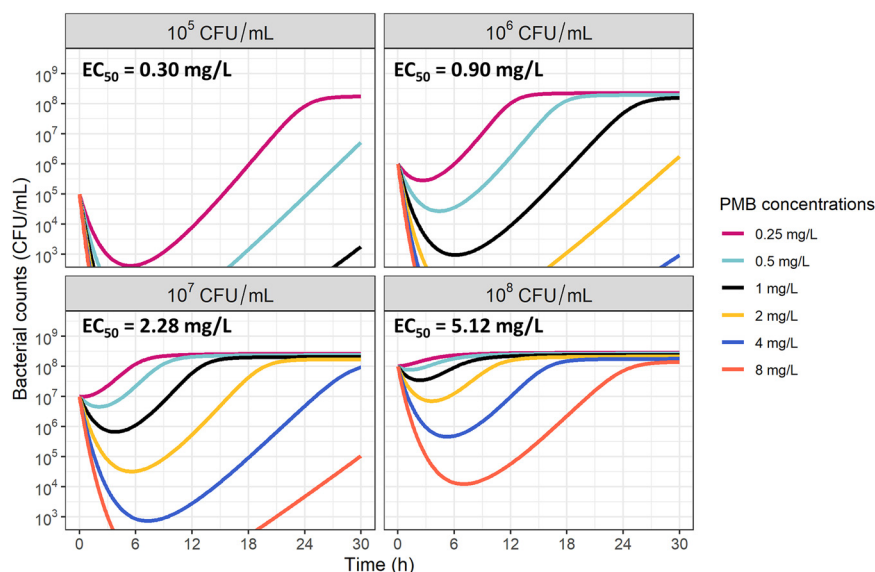


FIG 3 Simulations of expected bacterial counts (CFU/mL) versus time in the presence of various concentrations of PMB (pink: 0.25 mg/L; light blue, 0.5 mg/L; black, 1 mg/L; yellow, 2 mg/L; dark blue, 4 mg/L; and orange, 8 mg/L) for various starting inocula. EC_{50} corresponding to PMB concentration that results in 50% of $E_{max(0)}$.

confounding phenomenon that also contributes to these CFU versus time profiles, which therefore do not reflect exclusively that the PMB killing rate decreases when bacterial density increases. However, the initial killing rate, when bacteria are not yet adapted, can be used to characterize the IE specifically. It was derived from equation 1, using for each starting inoculum the corresponding EC_{50} value, and converted into the more explicit initial killing half-lives (IK-HL) (Table 2). As expected, the highest PMB concentrations lead to the shortest IK-HL. But more interestingly this modeling suggests that the IE is attenuated at high PMB concentrations. As an example, at a PMB concentration equal to 8 mg/L, IK-HL increased by 60% (from 5 to 8 min) when the starting inoculum increased from 10^5 to 10^8 , whereas at a PMB concentration of 0.25 mg/L, IK-HL increased by 380% (from 10 to 38 min) when the starting inoculum increased from 10^5 to 10^8 (Table 2). Noticeably, with adaptive resistance developing with time, the specific IE would be essentially observed at early times when the fraction of adapted bacteria is negligible or at least still limited, but in clinical practice, at these early times PMB concentrations are the highest, limiting the impact of IE. However, it should be reminded that this model was developed after *in vitro* experiments, presenting a number of advantages, such as the possibility of comparing a number of various inocula in a large range (10^5 to 10^8) as well as a large range of PMB concentrations (0.125 to 128 mg/L). These conditions are necessary for developing such a model combining IE and adaptive resistance but are not affordable for *in vivo* experiments. Yet the capability of this model to adequately describe IE *in vivo* remains to be assessed before extrapolating results of this present experiment to the clinical setting.

TABLE 2 Model derived initial killing half-lives (min) at various PMB concentrations and initial inocula

Inocula (CFU/mL)	Initial killing half-life (min) at PMB concn (mg/L) of:					
	0.25	0.5	1	2	4	8
10^5	10	8	7	6	5	5
10^6	15	11	9	7	6	6
10^7	24	17	13	10	8	7
10^8	38	26	18	13	10	8

As opposed to Bulitta et al., who developed a mechanistic model to describe the IE of *P. aeruginosa* on polymyxin E (or colistin) (18), the present model was developed without underlying mechanistic hypothesis. Yet it would have been of interest to explain this IE, but this was made difficult due to the remarkable genetic flexibility of *A. baumannii* (27). We simply tried to verify that AR and IE observed with this particular strain of *A. baumannii* in the presence of PMB were two distinct and unrelated phenomena, as implicitly considered in the model. The expression of seven genes (*lpxACD*, *pmrCAB*, and *wzc*) known to participate into *A. baumannii* adaptive resistance in the presence of PMB (28–32) was investigated, but no significant change was observed, regardless of the inoculum size (Fig. S2). Although regulation of other genes than those tested cannot be excluded, these experiments are consistent with the fact that AR developing with time depends upon PMB concentration but not of bacterial density. Lastly, although genetic changes are unlikely to occur repeatedly during 30-h TKC experiments, sequencing of the above-mentioned genes was performed, but no deletions or mutations were observed.

In conclusion, a PKPD model devoid of mechanistic rationale for IE, and distinguishing between IE and AR, has been successfully developed to characterize the *in vitro* IE of *A. baumannii* in the presence of PMB. This modeling approach is far more informative than comparing MICs values at different inocula. However, the capability of this new model to describe IE observed with other bacteria/antibiotics and resulting from various mechanism remains to be evaluated. *In vivo* evaluation of this IE observed *in vitro* also needs to be conducted.

MATERIALS AND METHODS

Chemicals and bacterial isolates. Polymyxin B (PMB), obtained from Sigma-Aldrich (Merck KGaA, Saint-Quentin Fallavier, France), was used to prepare fresh stock solutions of 10 mg/mL in sterile water. All chemicals and reagents used were analytical grade.

A clinical strain of *A. baumannii* (CS01), isolated from a patient with a meningitis before treatment with colistin, was used during this study (33).

Determination of PMB MICs. MICs were determined in triplicate based on the CLSI reference methods (34). Briefly, a suspension with an optical density (OD) of 0.1 to 0.15 (corresponding to 1×10^8 CFU/mL) of isolated colonies selected from an overnight culture on Mueller-Hinton agar (MHA) plate was prepared. This bacterial suspension was used to prepare inocula of 10^5 , 10^6 , 10^7 , or 10^8 CFU/mL in Muller-Hinton broth II cation adjusted (MHB) (bioMérieux, Marcy-l'Etoile, France). Then microdilutions of PMB were prepared in 96-well plates at concentrations ranging from 0.125 to 64 mg/L for each inoculum. The plates were incubated at $35 \pm 2^\circ\text{C}$ for 18 ± 2 h, and the MIC for each inoculum was recorded as the lowest drug concentration inhibiting visible bacterial growth. The results were confirmed by a resazurin reduction-based assay (35).

Time-kill kinetics curves (TKC) experiments. Bacteria were cultured in 5 mL of MHB with constant shaking (150 to 170 rpm) overnight at $35 \pm 2^\circ\text{C}$. This overnight suspension was diluted to 1/50 in MHB with a final volume of 10 mL and was incubated with constant shaking at 35°C during 2 h until an OD of 0.26 was achieved, corresponding to a bacterial density of 1×10^8 CFU/mL in exponential growth phase. This suspension was centrifuged at 3,000 g for 6 min and the pellet was resuspended in 1 mL of MHB to obtain a bacterial density of 1×10^9 CFU/mL. This suspension was used to prepare several inocula in MHB (20 mL) at concentrations of 10^5 , 10^6 , 10^7 , or 10^8 CFU/mL. PMB was added to the broth at various concentrations ranging from 0.125 to 4 mg/L for the 10^5 CFU/mL inoculum, from 0.25 to 16 mg/L for the 10^6 CFU/mL inoculum, from 0.5 to 32 mg/L for the 10^7 CFU/mL inoculum, and from 1 to 128 mg/L for 10^8 CFU/mL inoculum. Drug-free MHB was used as a positive control for each inoculum. These cultures were incubated at 37°C , with constant shaking and bacterial counts quantified after 0, 4, 8, 24, and 30 h by plating serial dilutions on MHA plates complemented with 1% active charcoal to prevent PMB carry-over effect (36). At time 0, each starting inoculum was also plated onto MHA plates containing PMB at a concentration of eight times the corresponding PMB MIC to determine quantitative viable counts of less-susceptible cells. CFU were counted after 24 h of incubation at 37°C (37). The limit of quantification was equal to 800 CFU/mL (i.e., $2.9 \log_{10}$ CFU/mL). Experiments were conducted in triplicate.

Pharmacodynamic model. TKC data obtained with the four inocula were simultaneously analyzed using NONMEM 7.4 (ICON plc, Dublin, Ireland) with the Laplacian algorithm and the M3 method for handling observations below the limit of quantification (38). The general structure of the model is detailed in the supplemental materials. Briefly, a previously developed semi-mechanistic model describing adaptive resistance was used (39). Different functions (linear, power, basic E_{\max} , or a sigmoidal E_{\max} function) for describing the PMB concentration-effect relationship and adaptive resistance were investigated. PMB was assumed to be stable over the course of the experiment as previously shown and, thus, no PK compartment was included in the model (40). Moreover, empirical functions (linear, exponential, or power function) and a mechanism-based model for characterizing the IE were assessed (24). Model selection was based on objective function value (OFV), relative standard errors (RSEs) of the parameter estimates,

and goodness of fit (GOF) plots (41). Visual predictive checks (VPCs) with stratification on PMB concentration and starting inoculum were drawn to evaluate the predictive performance of the model and taken into account for model selection. Observed bacterial counts were plotted versus time and overlaid with the median and 90% prediction interval obtained by simulating 1,000 replicates of the original data set. The concordance between simulations and observations was inspected visually.

Simulations of CFU versus time profiles. Simulations of expected PMB bactericidal effect at 0.25, 0.5, 1, 2, 4, and 8 mg/L as a function of time with all tested inocula were performed using R software (v.3.5.2) (42) with the *mrgsolve* R-package (v.0.10.0).

Quantification of the expression of PMB resistance genes and DNA sequencing. The expression of PMB resistance genes was quantified by a two-step reverse transcription-real-time PCR (RT-qPCR) method during TKC for starting inocula of 10^6 and 10^8 CFU/mL in presence or not of PMB at 1 mg/L with a final volume of 40 mL. The final protocol is detailed in the supplemental materials. Moreover, DNA sequences of the most likely resistance genes of *Acinetobacter baumannii* (*pmrA*, *pmrB*, *pmrC*, *lpxA*, *lpxC*, *lpxD*, and *eptA*) were analyzed after a whole genome sequencing according to a protocol presented in supplemental materials. Samples were taken over time at 0, 4, 8, and 24 h of the TKC.

SUPPLEMENTAL MATERIAL

Supplemental material is available online only.

SUPPLEMENTAL FILE 1, PDF file, 1 MB.

ACKNOWLEDGMENTS

The financial support of G. Akrong was provided by the Nouvelle Aquitaine Region and Inserm.

REFERENCES

1. Lenhard JR, Bulman ZP. 2019. Inoculum effect of β -lactam antibiotics. *J Antimicrob Chemother* 74:2825–2843. <https://doi.org/10.1093/jac/dkz226>.
2. Brook I. 1989. Inoculum effect. *Rev Infect Dis* 11:361–368. <https://doi.org/10.1093/clinids/11.3.361>.
3. López-Cerero L, Picón E, Morillo C, Hernández JR, Docobo F, Pachón J, Rodríguez-Bań J, Pascual A. 2010. Comparative assessment of inoculum effects on the antimicrobial activity of amoxicillin-clavulanate and piperacillin-tazobactam with extended-spectrum β -lactamase-producing and extended-spectrum β -lactamase-non-producing *Escherichia coli* isolates. *Clin Microbiol Infect* 16:132–136. <https://doi.org/10.1111/j.1469-0691.2009.02893.x>.
4. Bhagunde P, Chang K-T, Singh R, Singh V, Garey KW, Nikolaou M, Tam VH. 2010. Mathematical modeling to characterize the inoculum effect. *Antimicrob Agents Chemother* 54:4739–4743. <https://doi.org/10.1128/AAC.01831-09>.
5. Yokota S, Hakamada H, Yamamoto S, Sato T, Shiraishi T, Shinagawa M, Takahashi S. 2018. Release of large amounts of lipopolysaccharides from *Pseudomonas aeruginosa* cells reduces their susceptibility to colistin. *Int J Antimicrob Agents* 51:888–896. <https://doi.org/10.1016/j.ijantimicag.2018.02.004>.
6. Kesteman A-S, Ferran AA, Perrin-Guyomard A, Laurentie M, Sanders P, Toutain P-L, Bousquet-Mélou A. 2009. Influence of inoculum size and marbofloxacin plasma exposure on the amplification of resistant subpopulations of *Klebsiella pneumoniae* in a rat lung infection model. *Antimicrob Agents Chemother* 53:4740–4748. <https://doi.org/10.1128/AAC.00608-09>.
7. Mizunaga S, Kamiyama T, Fukuda Y, Takahata M, Mitsuyama J. 2005. Influence of inoculum size of *Staphylococcus aureus* and *Pseudomonas aeruginosa* on in vitro activities and in vivo efficacy of fluoroquinolones and carbapenems. *J Antimicrob Chemother* 56:91–96. <https://doi.org/10.1093/jac/dki163>.
8. Thomson KS, Moland ES. 2001. Cefepime, piperacillin-tazobactam, and the inoculum effect in tests with extended-spectrum β -lactamase-producing *Enterobacteriaceae*. *Antimicrob Agents Chemother* 45:3548–3554. <https://doi.org/10.1128/AAC.45.12.3548-3554.2001>.
9. Salas JR, Jaber-Douraki M, Wen X, Volkova VV. 2020. Mathematical modeling of the ‘inoculum effect’: six applicable models and the MIC advance-point concept. *FEMS Microbiol Lett* 367. <https://doi.org/10.1093/femsle/fnaa012>.
10. EUCAST. 2021. MIC determination of non-fastidious and fastidious organisms. EUCAST, Växjö, Sweden. https://eucast.org/ast_of_bacteria/mic_determination/.
11. CLSI. 2018. M07: methods for dilution antimicrobial susceptibility tests for bacteria that grow aerobically, 11th ed. CLSI, Wayne, PA. https://clsi.org/media/1928/m07ed11_sample.pdf.
12. Harada Y, Morinaga Y, Kaku N, Nakamura S, Uno N, Hasegawa H, Izumikawa K, Kohno S, Yanagihara K. 2014. In vitro and in vivo activities of piperacillin-tazobactam and meropenem at different inoculum sizes of ESBL-producing *Klebsiella pneumoniae*. *Clin Microbiol Infect* 20:O831–O839. <https://doi.org/10.1111/1469-0691.12677>.
13. Kim T, Lee SC, Bae M, Sung H, Kim M-N, Jung J, Kim MJ, Kim S-H, Lee S-O, Choi S-H, Kim YS, Chong YP. 2020. In vitro activities and inoculum effects of ceftazidime-avibactam and aztreonam-avibactam against carbapenem-resistant *Enterobacteriales* isolates from South Korea. *Antibiotics* 9:912. <https://doi.org/10.3390/antibiotics9120912>.
14. Adler A, Ben-Dalak M, Chmelnitsky I, Carmeli Y. 2015. Effect of resistance mechanisms on the inoculum effect of carbapenem in *Klebsiella pneumoniae* isolates with borderline Carbapenem resistance. *Antimicrob Agents Chemother* 59:5014–5017. <https://doi.org/10.1128/AAC.00533-15>.
15. Udekwi KI, Parrish N, Ankomah P, Baquero F, Levin BR. 2009. Functional relationship between bacterial cell density and the efficacy of antibiotics. *J Antimicrob Chemother* 63:745–757. <https://doi.org/10.1093/jac/dkn554>.
16. Nielsen EI, Khan DD, Cao S, Lustig U, Hughes D, Andersson DI, Friberg LE. 2017. Can a pharmacokinetic/pharmacodynamic (PKPD) model be predictive across bacterial densities and strains? External evaluation of a PKPD model describing longitudinal in vitro data. *J Antimicrob Chemother* 72:3108–3116. <https://doi.org/10.1093/jac/dkx269>.
17. Bulitta JB, Ly NS, Yang JC, Forrest A, Jusko WJ, Tsuji BT. 2009. Development and qualification of a pharmacodynamic model for the pronounced inoculum effect of Ceftazidime against *Pseudomonas aeruginosa*. *Antimicrob Agents Chemother* 53:46–56. <https://doi.org/10.1128/AAC.00489-08>.
18. Bulitta JB, Yang JC, Yohann L, Ly NS, Brown SV, D’Hondt RE, Jusko WJ, Forrest A, Tsuji BT. 2010. Attenuation of colistin bactericidal activity by high inoculum of *Pseudomonas aeruginosa* characterized by a new mechanism-based population pharmacodynamic model. *Antimicrob Agents Chemother* 54:2051–2062. <https://doi.org/10.1128/AAC.00881-09>.
19. Kalanuria AA, Ziai W, Zai W, Mirski M. 2014. Ventilator-associated pneumonia in the ICU. *Crit Care* 18:208. <https://doi.org/10.1186/cc13775>.
20. Garnacho-Montero J, Timsit J-F. 2019. Managing *Acinetobacter baumannii* infections. *Curr Opin Infect Dis* 32:69–76. <https://doi.org/10.1097/QCO.0000000000000518>.
21. Tam VH, Schilling AN, Vo G, Kabbara S, Kwa AL, Wiederhold NP, Lewis RE. 2005. Pharmacodynamics of Polymyxin B against *Pseudomonas aeruginosa*. *Antimicrob Agents Chemother* 49:3624–3630. <https://doi.org/10.1128/AAC.49.9.3624-3630.2005>.
22. Jacobs M, Grégoire N, Couet W, Bulitta JB. 2016. Distinguishing antimicrobial models with different resistance mechanisms via population

- pharmacodynamic modeling. *PLoS Comput Biol* 12:e1004782. <https://doi.org/10.1371/journal.pcbi.1004782>.
23. Nielsen EI, Friberg LE. 2013. Pharmacokinetic-pharmacodynamic modeling of antibacterial drugs. *Pharmacol Rev* 65:1053–1090. <https://doi.org/10.1124/pr.111.005769>.
 24. Nielsen EI, Cars O, Friberg LE. 2011. Predicting in vitro antibacterial efficacy across experimental designs with a semimechanistic pharmacokinetic-pharmacodynamic model. *Antimicrob Agents Chemother* 55:1571–1579. <https://doi.org/10.1128/AAC.01286-10>.
 25. Nielsen EI, Viberg A, Löwdin E, Cars O, Karlsson MO, Sandström M. 2007. Semimechanistic pharmacokinetic/pharmacodynamic model for assessment of activity of antibacterial agents from time-kill curve experiments. *Antimicrob Agents Chemother* 51:128–136. <https://doi.org/10.1128/AAC.00604-06>.
 26. Zavascki AP, Goldani LZ, Cao G, Superti SV, Lutz L, Barth AL, Ramos F, Boniatti MM, Nation RL, Li J. 2008. Pharmacokinetics of intravenous Polymyxin B in critically ill patients. *Clin Infect Dis* 47:1298–1304. <https://doi.org/10.1086/592577>.
 27. Wong D, Nielsen TB, Bonomo RA, Pantapalangkoor P, Luna B, Spellberg B. 2017. Clinical and pathophysiological overview of acinetobacter infections: a century of challenges. *Clin Microbiol Rev* 30:409–447. <https://doi.org/10.1128/CMR.00058-16>.
 28. Beceiro A, Llobet E, Aranda J, Bengoechea JA, Doumith M, Hornsey M, Dhanji H, Chart H, Bou G, Livermore DM, Woodford N. 2011. Phosphoethanolamine modification of Lipid A in colistin-resistant variants of *Acinetobacter baumannii* mediated by the pmrAB two-component regulatory system. *Antimicrob Agents Chemother* 55:3370–3379. <https://doi.org/10.1128/AAC.00079-11>.
 29. Trebosc V, Gartenmann S, Tötzl M, Lucchini V, Schellhorn B, Pieren M, Lociuo S, Gitzinger M, Tigges M, Bumann D, Kemmer C. 2019. Dissecting colistin resistance mechanisms in extensively drug-resistant *Acinetobacter baumannii* clinical isolates. *mBio* 10:e01083. <https://doi.org/10.1128/mBio.01083-19>.
 30. Lesho E, Yoon E-J, McGann P, Snesrud E, Kwak Y, Milillo M, Onmus-Leone F, Preston L, St Clair K, Nikolich M, Viscount H, Wortmann G, Zapor M, Grillot-Courvalin C, Courvalin P, Clifford R, Waterman PE. 2013. Emergence of colistin-resistance in extremely drug-resistant *Acinetobacter baumannii* containing a novel pmrCAB operon during colistin therapy of wound infections. *J Infect Dis* 208:1142–1151. <https://doi.org/10.1093/infdis/jit293>.
 31. Moffatt JH, Harper M, Harrison P, Hale JDF, Vinogradov E, Seemann T, Henry R, Crane B, Michael FS, Cox AD, Adler B, Nation RL, Li J, Boyce JD. 2010. Colistin resistance in *Acinetobacter baumannii* is mediated by complete loss of lipopolysaccharide production. *Antimicrob Agents Chemother* 54:4971–4977. <https://doi.org/10.1128/AAC.00834-10>.
 32. Campos MA, Vargas MA, Regueiro V, Llompant CM, Albertí S, Bengoechea JA. 2004. Capsule Polysaccharide mediates bacterial resistance to antimicrobial peptides. *Infect Immun* 72:7107–7114. <https://doi.org/10.1128/IAI.72.12.7107-7114.2004>.
 33. López-Rojas R, Jiménez-Mejías ME, Lepe JA, Pachón J. 2011. *Acinetobacter baumannii* resistant to colistin alters its antibiotic resistance profile: a case report from Spain. *J Infect Dis* 204:1147–1148. <https://doi.org/10.1093/infdis/jir476>.
 34. CLSI. 2020. MR01: polymyxin breakpoints for Enterobacteriales, *Pseudomonas aeruginosa*, and *Acinetobacter* spp., 2nd ed. CLSI, Wayne, PA. <https://clsi.org/standards/products/companion/companion/mr01/>.
 35. Lescat M, Poirel L, Tinguely C, Nordmann P. 2019. A resazurin reduction-based assay for rapid detection of polymyxin resistance in *Acinetobacter baumannii* and *Pseudomonas aeruginosa*. *J Clin Microbiol* 57:e01563. <https://doi.org/10.1128/JCM.01563-18>.
 36. Broussou DC, Toutain P-L, Woehrlé F, El Garch F, Bousquet-Melou A, Ferran AA. 2019. Comparison of in vitro static and dynamic assays to evaluate the efficacy of an antimicrobial drug combination against *Staphylococcus aureus*. *PLoS One* 14:e0211214. <https://doi.org/10.1371/journal.pone.0211214>.
 37. El Halfawy OM, Valvano MA. 2015. Antimicrobial heteroresistance: an emerging field in need of clarity. *Clin Microbiol Rev* 28:191–207. <https://doi.org/10.1128/CMR.00058-14>.
 38. Beal SL. 2001. Ways to fit a PK model with some data below the quantification limit. *J Pharmacokinet Pharmacodyn* 28:481–504. <https://doi.org/10.1023/A:1012299115260>.
 39. Mohamed AF, Cars O, Friberg LE. 2014. A pharmacokinetic/pharmacodynamic model developed for the effect of colistin on *Pseudomonas aeruginosa* in vitro with evaluation of population pharmacokinetic variability on simulated bacterial killing. *J Antimicrob Chemother* 69:1350–1361. <https://doi.org/10.1093/jac/dkt520>.
 40. Orwa JA, Govaerts C, Gevers K, Roets E, Van Schepdael A, Hoogmartens J. 2002. Study of the stability of polymyxins B1, E1 and E2 in aqueous solution using liquid chromatography and mass spectrometry. *J Pharmaceutical and Biomedical Analysis* 29:203–212. [https://doi.org/10.1016/S0731-7085\(02\)00016-X](https://doi.org/10.1016/S0731-7085(02)00016-X).
 41. Nguyen THT, Mouksassi M-S, Holford N, Al-Huniti N, Freedman I, Hooker AC, John J, Karlsson MO, Mould DR, Ruixo JJP, Plan EL, Savic R, Hasselt JGC, van Weber B, Zhou C, Comets E, Mentré F, Model Evaluation Group of the International Society of Pharmacometrics (ISoP) Best Practice Committee. 2017. Model evaluation of continuous data pharmacometric models: metrics and graphics. *Cpt Pharmacometrics Syst Pharmacol* 6:87–109. <https://doi.org/10.1002/psp4.12161>.
 42. R Core Team. 2021. A language and environment for statistical computing. R Foundation for Statistical Computing, Vienna, Austria. Available online at <https://www.R-project.org/>.